Fingerprints of Superpositions of Multifractals and Second Order Phase Transitions

Ruedi Stoop

Institut für Neuroinformatik, ETHZ / Universität Zürich
Gloriastr.32, CH-8006, Zürich

Z. Naturforsch. **52 a,** 393–397 (1997); received December 19, 1996

The generic model of superimposed multifractal measures is discussed from the generalized entropy point of view. Natural conditions for the existence of second order critical lines are given. The second order phase transitions may manifest themselves in stopping points of the entropy-like thermodynamic functions. The findings are of experimental relevance.

PACS numbers: 05.45.+b, 05.70.Fh, 61.43.Hv, 05.50.+q

As a consequence of the success of nonlinear dynamics, the theory of fractals [1 - 5] has attracted much interest. Singular measures of multifractal [6] structure were shown to characterize strange attractors [7], diffusion [8, 9], scattering processes [4, 10], turbulence, fractal diffusion-limited aggregation [3], etc. Later it was found that relations exist to already well-known fields of physics. As an example, in the analysis of multifractals one may take advantage of a (formal) equivalence of multifractals with spin systems investigated in statistical mechanics [11]. In analogy to the latter, thermodynamic quantities are defined and nonanalytic behavior of these functions can be interpreted as phase transition phenomena [12]. The purpose of this contribution is to provide an exemplary discussion of a model [13] in which a generic mechanism for second order phase transitions is observed. Then, the appearance of stopping points in the thermodynamic functions derived from experiments is related to the latter phenomenon.

Often in experiments the full multifractal structure of the object cannot be accessed. What can be measured is a fractal structure with a measure on it. In this way, a generalized fractal with a support-independent measure is obtained (in contrast to the monovariate thermodynamic formalism, where length scales and measures can all be expressed by the length scales alone). The example of the diffusion on a grid of identical cells [9] indicates the wide applicability of this concept for biology and chemistry. As a probably more well-known example we may think of the result stemming from a generalized Baker map [7]. In addition, it may be useful to consider two or more different sources contributing to the measure imposed on the fractal structure. Using baker maps, this can be generated by a superposition of two maps with different sets of probabilities $p_i, i = 1..C$ (where $C = 2$ for binary, $C = 3$ for ternary Cantor sets, etc.), but with identical sets of length scales l_i. From the experimental point of view, the situation corresponds to two sources generating essentially overlapping Cantor structures with measure. The question then arises how the independent measures combine to make the common thermodynamic functions.

As a starting point, a related question was probably first considered in [14]. A thorough discussion of superimposed Cantor sets was then first given in [13], followed by a discussion of a special case of second order phase transition [15]. In the present contribution we enlighten in full generality the generic situation, which will be defined as the superposition of two probability measures on a three-scale Cantor support. We discuss the problem from a new point of view which allows a connection of the second order phase transitions to commonly measured quantities. By adopting the generalized entropy [16, 17] point of view we extend our knowledge on first and second order transitions occurring in this context.

Let us first introduce the two sources which will contribute to the combined system, then we will present the numerical result for the free energy of the combined system. We end by discussing the generalized entropy function, which will allow a more

Reprint requests to Dr. R. Stoop, Fax: +41 2576983.

0932-0784 / 97 / 0500-0393 $ 06.00

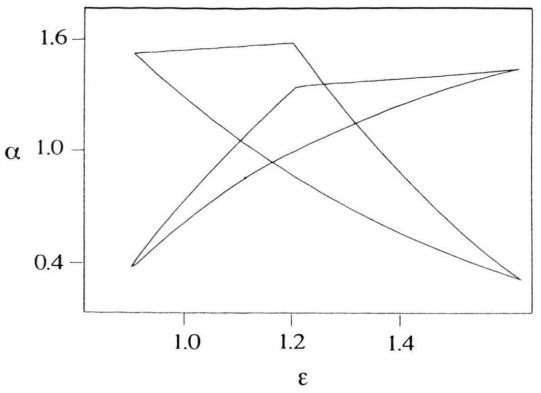

Fig. 1. Support of the generalized entropy function $S(\alpha, \varepsilon)$ of two three-scale Cantor sets with measure. The fact that the same set of length scales is used is mirrored by corresponding ε-values of the corner points. Parameters: $p_1 = 0.1$, $p_2 = 0.2$, $p_3 = 0.7$ (measure of the first source), $p_{1s} = 0.6$, $p_{2s} = 0.15$, $p_{3s} = 0.25$ (measure of the second source), $l_1 = 0.2$, $l_2 = 0.3$, $l_3 = 0.4$ (length scales of the Cantor set).

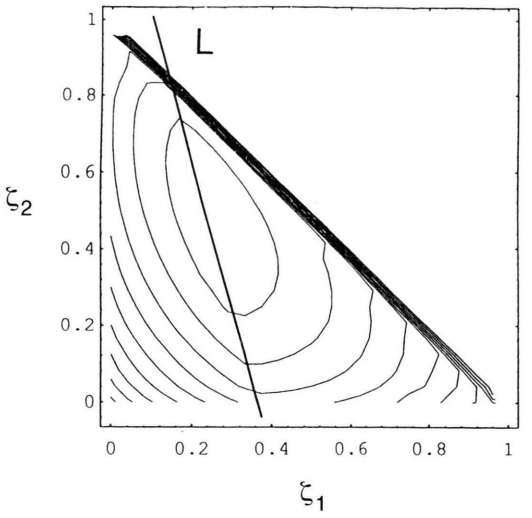

Fig. 2. $g(\boldsymbol{\xi}, q, \beta)$ for an exemplary (q, β)-pair showing the realization of the minimum on the line L (phase 3).

condensed insight into the properties displayed by such systems. Let us start from the two isolated Cantor sets with measure. The setting for our example is that we have $M = 2$ sources contributing to the measure of the $C = 3$-scale Cantor support. It will be argued that this is the relevant case to be considered. In Fig. 1 we show the associated supports of the generalized entropy functions, i. e. the range of the scaling exponents of the isolated systems. The variable ε describes the exponent generated by the scaling of the support (i. e. by the length scales l_i), the variable α describes the local dimensions the system can produce [3]. If j denotes a periodic address in the symbolic representation of the Cantor set, we have $\varepsilon = \frac{1}{N} \mid \ln(l_j) \mid$ and $\alpha = \frac{\ln(p_j)}{\ln(l_j)}$. Note that the corner points of the support indicate the properties of the periodic addresses of period 1, and that by changing the length scales we may force α into the interval $[0, 1]$ without changing the nature of the system. For the combined or superposed system the free energy is then given by the minimum of the individual free energies. Taking into consideration that asymptotically the two contributions to the measure have to be of the same order, the partition function Z of the N-th hierarchic level is written as [13]

$$Z_N(q,\beta) = \sum_{j=0}^{N} \sum_{k=0}^{N-j} T_N(j,k) \left[\sum_{\nu=1}^{M} \pi(\nu) p_1(\nu)^j p_2(\nu)^k p_3(\nu)^{N-j-k} \right]^q \left[{l_1}^j {l_2}^k {l_3}^{N-j-k} \right]^\beta . \quad (1)$$

For large N we have the behavior

$$Z_N(q,\beta) \sim \int_0^1 d\xi_1 \int_0^{1-\xi 1} \mathrm{d}\xi_2 \exp\{-N[q a_p(\xi_1,\xi_2) + \beta a_l(\xi_1,\xi_2) - s_T(\xi_1,\xi_2)]\} \quad (2)$$

with $s_T(\xi_1,\xi_2) = -\xi_1 \ln \xi_1 - \xi_2 \ln \xi_2 - \xi_3 \ln \xi_3$,

$$a_p(\xi_1,\xi_2) = \min_\nu a_{p\nu}(\xi_1,\xi_2) = \min_\nu [-\xi_1 \ln p_1(\nu) - \xi_2 \ln p_2(\nu) - \xi_3 \ln p_3(\nu)] \quad (3)$$

and $a_l(\xi_1,\xi_2) = -\xi_1 \ln l_1 - \xi_2 \ln l_2 - \xi_3 \ln l_3$.

The parameters $\pi(\nu), \nu = 1, 2$, are the weights of the contributions of the two sources ($\sum_\nu \pi(\nu) = 1$), and $\xi_1 = j/N$, $\xi_2 = k/N$ and $\xi_3 = (N - j - k)/N$ are the densities of the digits '1, 2, 3', respectively, in the ternary address of the fractal elements [3]. $T_N(j,k)$ are the trinomial coefficients. For our numerical example, the function

$$g(\boldsymbol{\xi}, q, \beta) = q a_p(\xi_1,\xi_2) + \beta a_l(\xi_1,\xi_2) - s_T(\xi_1,\xi_2) \quad (4)$$

looks for a characteristic (q, β)-pair as shown in Figure 2. Line L separates the region to which the

minimum of the *contribution 1* is confined (area left to the line) from the region in which the *contribution 2* must assume its minimum. The line itself represents the equality of the two contributions $a_{p1}(\xi_1, \xi_2) = a_{p2}(\xi_1, \xi_2)$, from which the equation $\xi_2 = f[\xi_1, p_1, p_2, p_{1s}, p_{2s}] := \ln[(1 - p_{1s} - p_{2s})/(1 - p_1 - p_2)] - \xi_1 \ln[(p_1/p_{1s})(1 - p_{1s} - p_{2s})/(1 - p_1 - p_2)]/\ln[(p_2/p_{2s})(1 - p_{1s} - p_{2s})/(1 - p_1 - p_2)]$ for the line may be derived easily (for convenience we use the index s to indicate the contributions from the second source). Accordingly, we have three different phases: Either the minimum of $g(\boldsymbol{\xi}, q, \beta)$ is a proper critical point, then it can be located in the region characteristic for contribution 1 or 2, or it is situated on the border between the two regions. In this third case (*'phase 3'*) the minimum is assumed at the critical point of g restricted to L. In the case of two-scale Cantor sets, the minimum line L degenerates to a peak point, a situation which is characterized by vanishing finite-N fluctuations of ξ around the saddle point ('quenched' phase [15] with vanishing second derivatives). Whereas for the two-source two-scale Cantor system almost all results are analytical (see [13]), for $C > 2$ they have to be determined numerically. Note that for more complicated systems than our two-source three-scale Cantor system even more general kinds of minima may be present, from where additional second order transitions may follow.

Free energy

From g, the free energy function $F(q, \beta) = \lim_{N\to\infty} \frac{1}{N} \ln(Z_N(q, \beta))$ is easily derived. In Fig. 3, a contour plot of the free energy shows the three phases and the associated critical lines. Crossing the border between phase 1 and phase 2 induces a first order transition, crossing a border involving phase 3 induces a transition of second order. Upon variation of β for $q > 0$ one always observes a first order transition between phase 1 and phase 2. In the most popularly observed specific entropy function $f(\alpha)$, this transition always takes place at ($q = 1, \beta = 0$). Phase 3, which is born at $q = 0$, may, however, not be detectable by $f(\alpha)$ since the zero-line of the free energy may pass by its border. In [13] a geometrical explanation for the existence/nonexistence of the second order transition in the $f(\alpha)$-function was given for two-scale Cantor sets. In our more general setting, the reasoning is similar, but the presentation is different and the emphasis is on generic results.

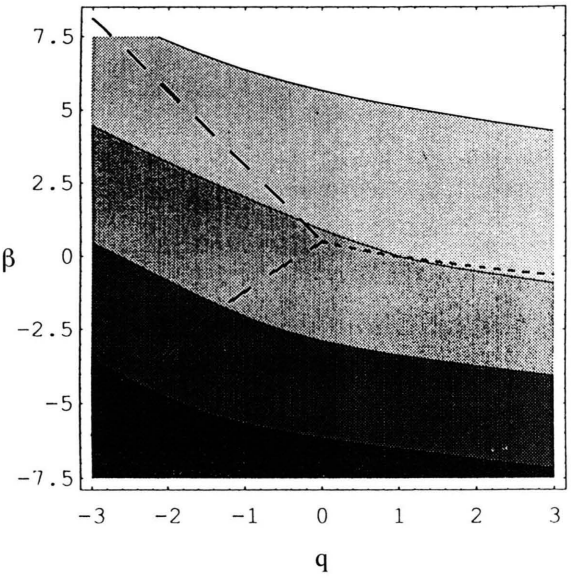

Fig. 3. Contour plot of the free energy with the three phases. Short dashes: first order transition line, long dashes: second order transition line. The second contour line from top corresponds to $F(q, \beta) = 0$.

Generalized entropy

The most condensed way to present the general information on the scaling behavior of a system is with the help of the generalized entropy function $S(\alpha, \varepsilon) = \max_{q,\beta}[F(q, \beta) + \varepsilon\beta + \varepsilon\alpha q]$ (where ε is chosen as a positive quantity). In Fig. 4 we show a contour plot of S for our system. Observe that the maximum value of S (i. e., $\ln(C)$, where $C = 3$) is assumed by the topological entropy and that the maximal values on the border are given by the value $\ln(2)$, because there the entropy function is determined by orbits generated from $c = 2$ symbols. It is instructive to see how the individual entropy functions (compare Fig. 1) are forced to merge under the conditions for superposition. The rule which is obeyed is the following: Imagine the system being parameterized by its C-nary addresses. Comparing the contributions from the two subsystems, it is seen that the contribution with the smaller α-scaling index survives in the limit $N \to \infty$. Therefore, upper part wings are clipped while the lower ones remain. As a consequence, the point with the highest α-value will be found at the end of one wing or on the intersection of the two supports. In the second case, the value of the general-

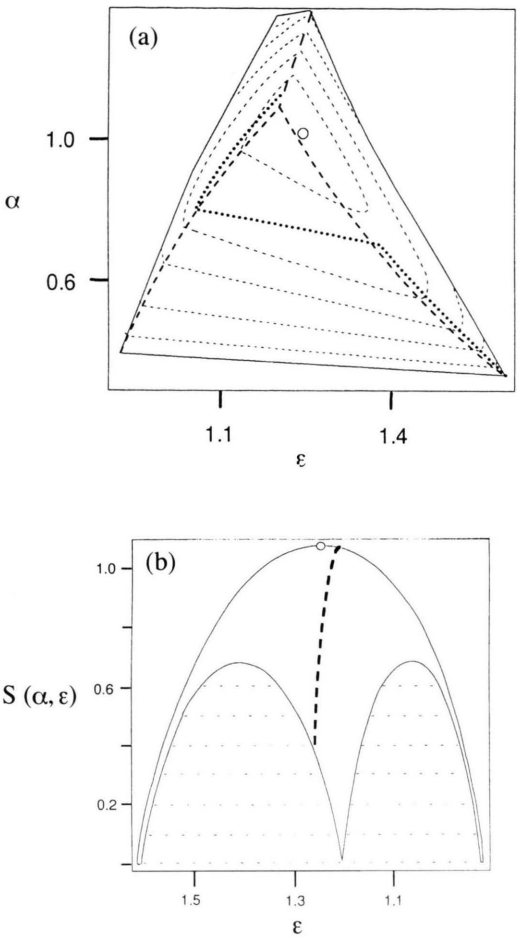

Fig. 4. a) Support of $S(\alpha, \varepsilon)$ for the combined multifractal measures. Light dashes: contour lines; long fat dashes: second order transition line; short fat dashes: first order transition line. Circle: location of the topological entropy; dotted: trace along which $f(\alpha)$ is evaluated. b) Generalized entropy function $S(\alpha, \varepsilon)$ viewed from high α-values. The light dashes indicate the contour lines of the first order transition region.

ized entropy function will be nonzero. For the 2-scale problem we obtain an intersection point, therefore phase 3 is linear, whereas for 3-scale problems we obtain an intersection line and phase 3 is not linear. As a consequence, for 2-scale systems a finite q-value is characteristic for phase 3. For the 3-scale problem, phase 3 is usually entered at a finite q-value but the phase can be followed for decreasing q values, reaching the border for $q = -\infty$ only. Figure 4 illustrates these properties.

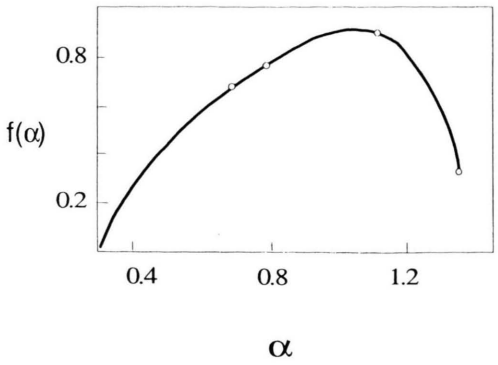

Fig. 5. $f(\alpha)$-curve associated with Figure 4. Circles mark the border of first and second order transition regimes.

Specific entropies

The specific entropy functions which can be measured in experiments are [4, 7] $f(\alpha)$ [6], $S(\varepsilon) = S(\alpha, \varepsilon)\,|_{q=0}$ [18, 19], $\phi(\lambda) = S(\alpha, \varepsilon)\,|_{q=1}$ (provided that a convenient definition of the dynamical probability is taken) [20] and $g(\Lambda) = S(\alpha, \varepsilon)\,|_{\beta=0}$. Below we sketch the behavior of these functions. $S(\varepsilon)$ probes the whole ε-range. Passing through the bicritical point and through the topological entropy, the first order transition region is avoided and phase 3 is only touched in the bicritical point. $\phi(\lambda)$ also starts on the left wing, continues to climb up this side until below the bicritical point the first order critical line is reached and a jump to the right wing is made. Without witnessing a second order transition, $\phi(\lambda)$ finally reaches the lowest point on the right wing. $f(\alpha)$ starts on the right wing, undergoes a first order transition at a small α-value and follows the left wing up until reaching phase 3 and ending at the point of the second order critical line at nonzero entropy. There, the derivative of the curve is infinite. $g(\Lambda)$ starts on the left wing of the entropy function, performs a first order transition to the right-hand wing from where the function reaches the second order critical line which it follows up to the top border. From Fig.4, many of the discussed features can immediately be read off and the behavior of these functions can readily be estimated. As an illustration we show in Fig. 5 $f(\alpha)$.

Multifractals with $M > 2$, $C > 3$, or grammatical restrictions

If more than two Cantor sets are present, by the described mechanism typically a star-like structure of

phases inducing second order transitions will evolve. At intersection points peaks may appear which correspond to quenched phases. However, unlike the two-system two-scale case, there will not be a quenched phase at the end of the spectrum. For $C > 3$, phases inducing second order transitions may appear which are no longer 1-dimensional. For high enough α-values, however, they will generically end up in 1-dimensional curves. In the presence of grammatical restrictions, the situation remains essentially the same with the exception that the number of corner points of the entropy functions corresponding to the individual Cantor sets generally change [21]. Note that their maximal number is limited by the number of primitive orbits needed for the cycle expansion of the system [22].

Experimental verification of second order phase transitions

On the basis of the above findings we conclude that superpositions of Cantor structures are likely to show up as stopping points of specific entropy functions measured in experiments. Whether it will be possible to distinguish between a finite and an infinite derivative at the stopping point seems doubtful, since the error bars on the right hand side of the characteristic hump of the specific entropy functions are generally large. However, a distinction between second order transition effects and degenerate systems which may produce similar results [6, 17] may be possible by measuring more than one specific entropy function, since in many of the latter cases the effect is due to a degeneracy which may be forced to disappear by switching to another specific entropy function [23].

In conclusion, we have presented a new approach, shown new features and new numerical results for the most general situation where first order and second order phase transitions appear together in the thermodynamics of multifractals. Since the superposition of multifractals is a natural mechanism, we expect that our results can be observed in experiments. In order to improve the knowledge on an experimental system, the information that the system is compatible with a projection of two or several sources on a single fractal structure may be significant. Fig. 4 then indicates, what kind of relationships between observable specific entropy functions may be expected. Furthermore, an alternative explanation for the common difficulty to measure full $f(\alpha)$ curves is given [24].

Acknowledgements

Stimulating discussions with G. Radons are gratefully acknowledged. This work was partially supported by the Swiss National Science Foundation.

[1] B. B. Mandelbrot, The Fractal Geometry of Nature, W. H. Freeman, New York 1982.
[2] K. Falconer, Fractal Geometry, J.Wiley and Sons, Chichester 1990.
[3] J. Feder, Fractals, Plenum, New York 1988.
[4] T. Tél, Transient Chaos, World Scientific, Singapore 1991.
[5] H. G. Schuster, Deterministic Chaos, 2nd ed. VCH, Weinheim 1989.
[6] T. C. Halsey, M. H. Jensen, L. P. Kadanoff, I. Procaccia, and B. Shraiman, Phys. Rev. A **33**, 1141 (1986).
[7] J. Peinke, J. Parisi, O. E. Roessler, and R. Stoop, Encounter with Chaos, Springer, Berlin 1992.
[8] R. Artuso, G. Casati, and D. L. Shepelyanski, Phys. Rev. Lett. **68**, 3826 (1992); R. Ketzmerick, G. Petschel, and T. Geisel, Phys. Rev. Lett. **69**, 695 (1992); I. Guarneri and G. Mantica, Phys. Rev. Lett. **73**, 3379 (1994).
[9] R. Artuso, Phys. Lett. A **160**, 530 (1991); X.-J. Wang and C.-K. Hu, Phys. Rev. E **48**, 728 (1993); R. Stoop, Europhys. Lett. **25**, 99 (1994); R. Stoop, Europhys. Lett. **29**, 433 (1995).
[10] C. Godrèche and J. M. Luck, J. Phys. A., Math. Gen. **23**, 3769 (1990); F. Axel and H. Terauchi, Phys. Rev. Lett. **66**, 2223 (1991).
[11] See e. g.: C. J. Thompson, Classical Equilibrium Statistical Mechanics, Clarendon Press, Oxford 1988.
[12] D. Katzen and I. Procaccia, Phys. Rev. Lett. **58**, 1169 (1987), and refs. therein; E. Ott, C. Grebogi, and J. A. Yorke, Phys. Lett. A **135**, 343 (1989).
[13] G. Radons and R. Stoop, J. Stat. Phys. **82**, 1063 (1996).
[14] G. Radons, Z. Naturforsch. **49a**, 1219 (1994).
[15] G. Radons, Phys. Rev. Lett. **75**, 2518 (1995).
[16] M. Kohmoto, Phys. Rev. A **37**, 1345(1988); J. Peinke, J. Parisi, O. E. Roessler, and R. Stoop, Encounter with Chaos, Springer, Berlin, 1992; Z. Kovács and T. Tél, Phys. Rev. A **45**, 2270 (1992).
[17] T. Tél, Z. Naturforsch. **43a**, 1154 (1988).
[18] J.-P. Eckmann and I. Procaccia, Phys. Rev. A **34**, 659 (1986).
[19] P. Széphalusy and T. Tél, Phys. Rev. A **34**, 2520 (1986).
[20] R. Stoop and J. Parisi, Phys. Rev. A **43**, 1802 (1991).
[21] R. Stoop and J. Parisi, Physica D **58**, 325 (1992).
[22] R. Artuso, E. Aurell, and P. Cvitanović, Nonlinearity **3**, 361 (1990).
[23] R. Stoop, unpublished.
[24] Usually, the lack of statistics is blamed for such an effect (see also [21]).